Application of physics-informed neural networks in solving temperature diffusion equation of seawater

Lei HAN(NUIST, China), Changming DONG(NUIST, China), Yusuke UCHIYAMA(Kobe Univ.)

BACKGROUND

- **Partial Differential Equations (PDEs)**
  Fundamental models in physics, engineering, economics and biology for describing spatial–temporal processes.
  Traditional solvers (finite difference/element/volume) discretize domains into millions of grids, leading to high computational cost.
- **Physics-Informed Neural Networks (PINNs)**
  Encode PDE residuals + boundary/initial conditions into a neural-network loss function.
  Enable data-driven, mesh-free solutions for both forward (known PDE → solution) and inverse (unknown parameters → learned) problems.
- **Seawater Temperature Diffusion**
  Governs ocean heat transport, currents, and climatic interactions.
  Boundary conditions (Dirichlet: fixed SST; Neumann: surface heat flux; Robin: mixed) critically affect solution stability and accuracy.
- **Gap & Contribution**
  Existing PINN studies apply to heat conduction but lack side-by-side comparisons under Dirichlet/Neumann/Robin conditions and sensitivity to observation number/location.

  This work:
  1. Compares PINN performance for forward/inverse seawater diffusion under three boundary-condition types.
  2. Examines loss-term weighting effects.
  3. Assesses how observation density and placement influence solution and parameter recovery.
  4. Validates methods with Argo profiles in the north-central Pacific.

METHODS

Simplified Seawater Temperature Diffusion

- Assumption: Horizontal advection is negligible → vertical diffusion dominates.
- Governing equation: $\frac{\partial T}{\partial t} = \frac{\partial}{\partial z}\left(k_z \frac{\partial T}{\partial z}\right)$

where T is the seawater temperature, t is time, z is the vertical coordinate, and k_z is the vertical temperature diffusion coefficient.

PINNs Framework

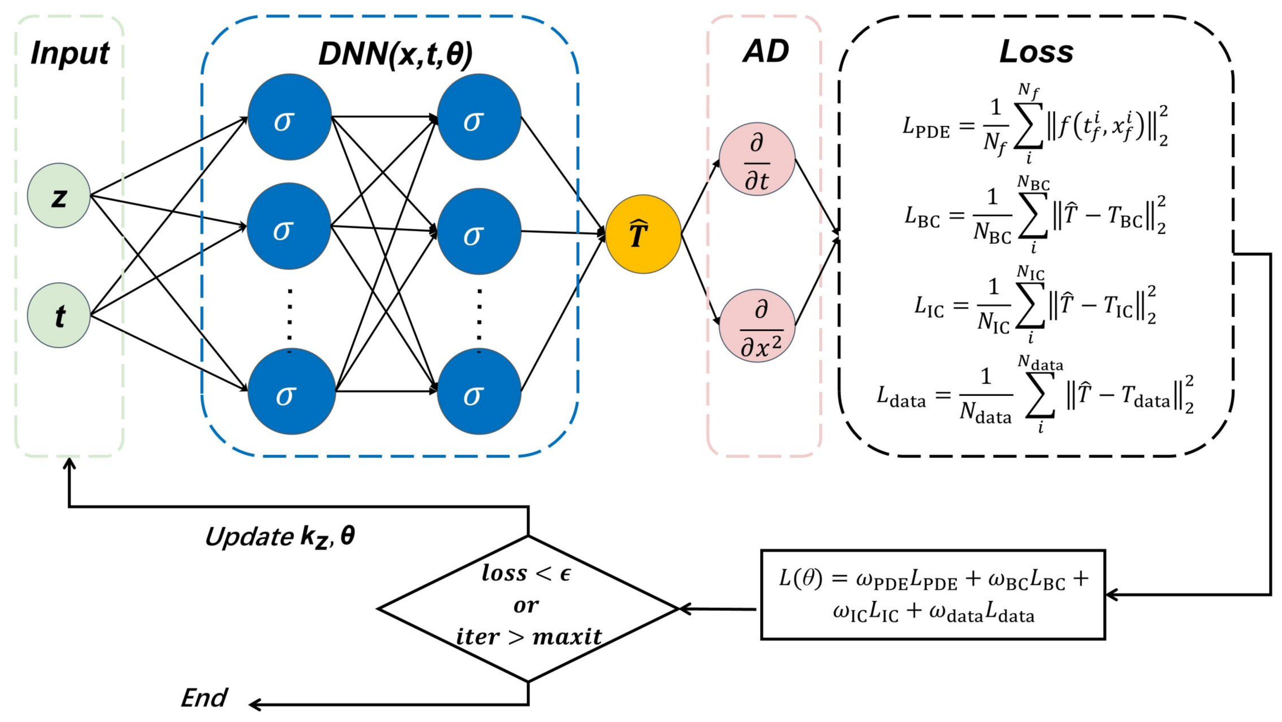

Fig. 1 Schematic of PINN training, showing PDE, BC, IC and data-driven loss components.

RESULTS

Boundary-Condition Scenarios

Dirichlet (Fixed-T):

$$\begin{cases} \frac{\partial T}{\partial t} = k_z \frac{\partial^2 T}{\partial z^2} & 0 < z < L,\ t > 0 \\ T(z,0) = \sin\frac{\pi z}{2} + \sin \pi z & 0 \le z \le L \\ T(0,t) = 0, T(L,t) = 0 & t > 0 \end{cases}$$

Neumann (No-Flux):

$$\begin{cases} \frac{\partial T}{\partial t} = k_z \frac{\partial^2 T}{\partial z^2}, & 0 < z < L, t > 0 \\ T(z,0) = \cos\frac{\pi z}{2} + \cos \pi z & 0 \le z \le L \\ T_z(0,t) = 0, T_z(L,t) = 0, & t > 0 \end{cases}$$

Robin (Mixed):

$$\begin{cases} \frac{\partial T}{\partial t} = k_z \frac{\partial^2 T}{\partial z^2} & 0 < z < L, t > 0 \\ T(z,0) = e^{-z} + \frac{\pi}{2}\cos\frac{\pi z}{2} - \sin\frac{\pi z}{2} + \pi \cos \pi z - \sin \pi z & 0 \le z \le L \\ T(0,t) + hT_z(0,t) = 0, T(L,t) + hT_z(L,t) = 0 & t > 0 \end{cases}$$

Table 1 Error metrics for the solution of forward and inverse problems of the temperature diffusion equation under three boundary conditions using PINN.

Instances	Mean PDE Residual ($\times 10^{-5}$)	L2 Relative Error ($\times 10^{-5}$)	MAE ($\times 10^{-6}$)	k_z Absolute Error ($\times 10^{-7}$)
DE_Dir_FWD	3.6585±0.7259	1.9540±0.2034	5.5912±1.5139	-
DE_Neum_FWD	3.1366±0.9654	1.7306±0.5565	5.3412±2.8130	-
DE_Rob_FWD	17.135±6.0176	3.4923±1.5377	25.697±19.063	-
DE_Dir_INV	6.9700±1.8656	3.3431±1.2058	10.163±1.4692	3.6295±2.1385
DE_Neum_INV	7.6856±1.2273	4.1509±0.7079	9.7766±3.5303	3.7775±2.5635
DE_Rob_INV	17.347±5.3748	2.9369±1.5615	20.207±16.128	8.0050±4.6345

RESULTS

Sensitivity of Loss-Function Weights

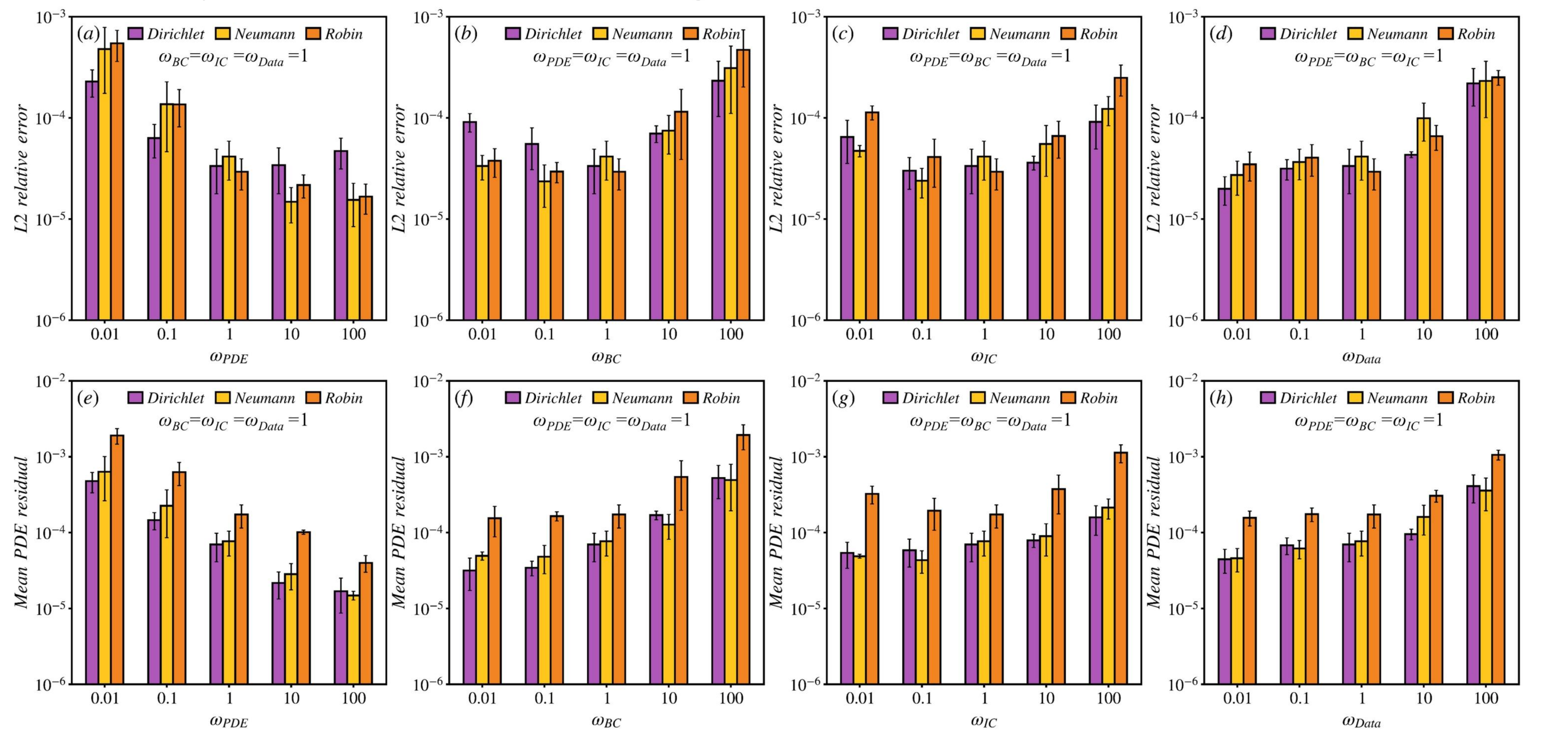

Fig.2 L2 relative error (a)-(c) and mean PDE residual (d)-(f) for experiments with different loss function weighting coefficients in the solution of the inverse temperature diffusion equation.

Key Findings:

- **PDE weight:** Raising from 0.01→10 steadily cuts L_2 error & mean residual. Beyond 10→100, gains plateau—and under Dirichlet even reverse, as BC/IC get under-emphasized.
- **BC/IC weights:** Little effect up to 1; errors spike sharply when ≥10 (over-penalizing boundaries or initial conditions).
- **Data weight:** Mirrors BC behavior: optimal near 1, large values (≥10) degrade both error and residual.

RESULTS

PINNs Inversion of Vertical Seawater Temperature Diffusion

Source: Argo GDAC profiles (2011–2020)

Regions:

23–27° N, 163–166° W (shallow, rugged bathymetry)

23–27° N, 166–169° W (deep, flat seabed; mean depth > 4 000 m)

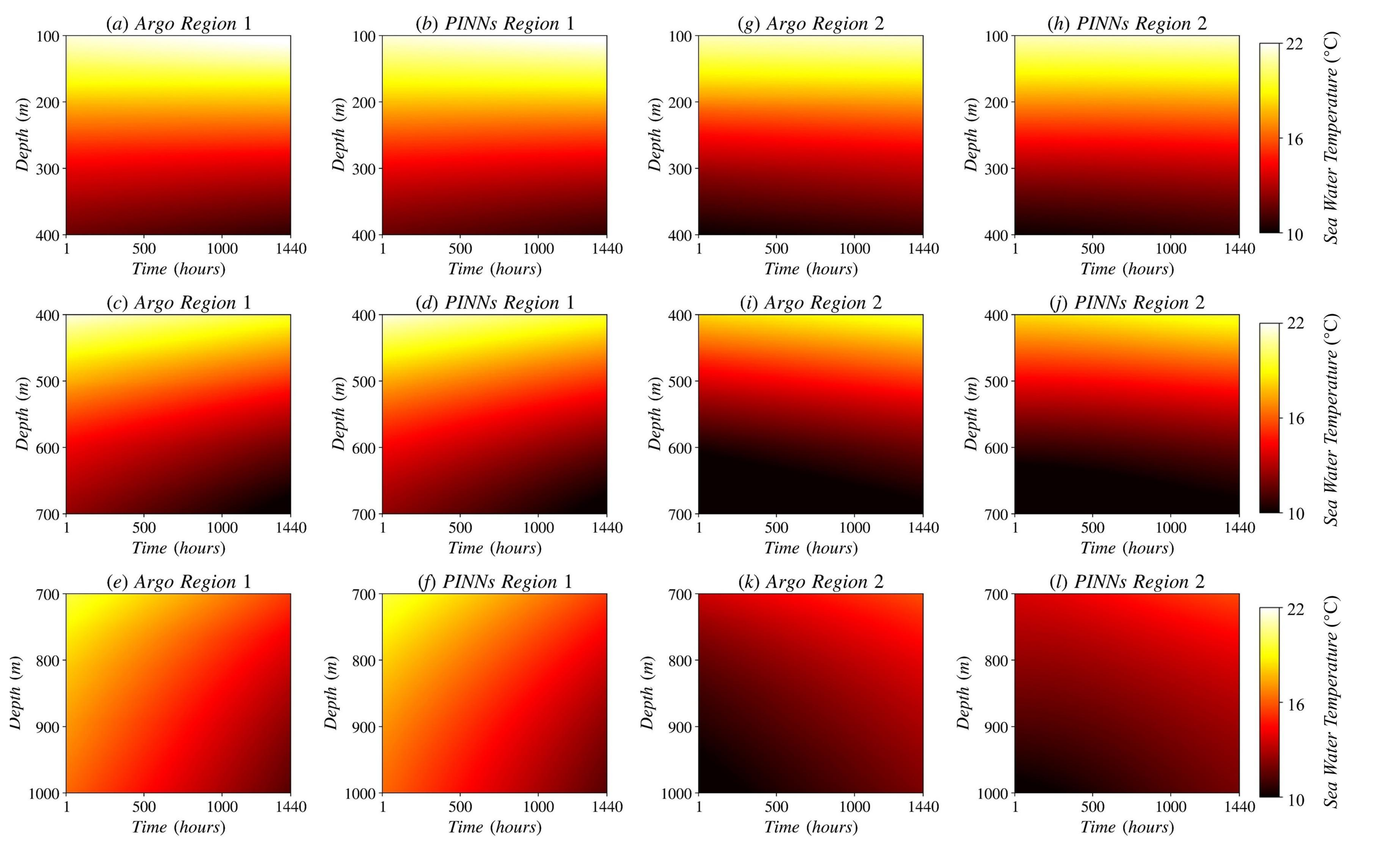

Fig.3 Comparison of PINNs inverted seawater temperature and Argo observations at different depths in regions 1 and 2 during spring.

Vertical structure:

Both regions: PINNs accurately reconstruct Argo temperature profiles over time

Upper 400 m: relatively slow changes; below 400 m: stronger temporal variability

Topography effect:

No degradation in inversion quality for either rugged (Region 1) or flat (Region 2) seabed

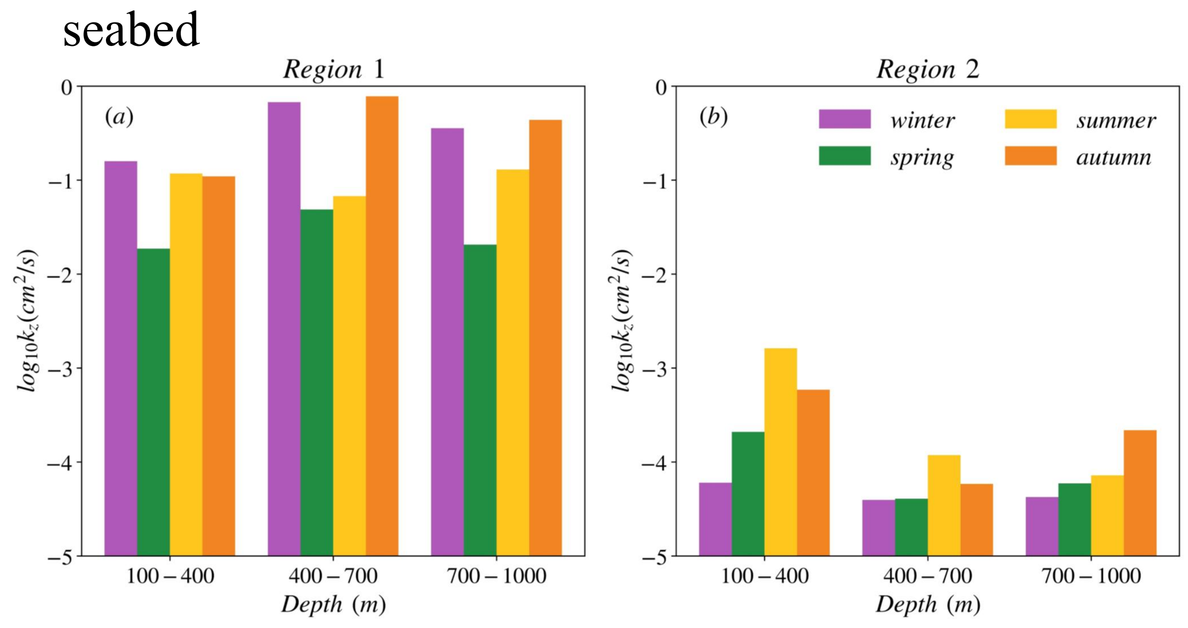

Fig.4 Estimated temperature diffusion coefficients at different depths across four seasons in regions 1 and 2

Region 1: higher than Region 2, peaking in autumn/winter due to convective cooling and internal-tide mixing.

Region 2: lower, nearly constant year-round, reflecting limited energy input variations.

CONCLUSIONS

- PINNs reliably solve forward/inverse seawater diffusion, with highest accuracy under Dirichlet/Neumann conditions.
- Argo validation over 2011–2020 shows mean errors ≲ 10^{-3} across depths, seasons, and varied bathymetry.
- Recommendation: use Dirichlet (fixed SST) setups for best convergence; PINNs excel in sparse-data ocean PDE problems.